The Plant Journal (2003) **35**, 1–15 doi: 10.1046/j.1365-313X.2003.01775.x

The dynamin-like protein ADL1C is essential for plasma membrane maintenance during pollen maturation

Byung-Ho Kang, David M. Rancour and Sebastian Y. Bednarek*
Department of Biochemistry, University of Wisconsin-Madison 433 Babcock Dr., Madison, WI 53706, USA

Received 19 January 2003; revised 7 March 2003; accepted 16 March 2003.
*For correspondence (fax +1 608 262 3453; e-mail bednarek@biochem.wisc.edu).

Summary

Dynamin-related GTPases regulate a wide variety of dynamic membrane processes in eukaryotes. Here, we investigated the function of ADL1C, a member of the *Arabidopsis* 68 kDa dynamin-like protein family. Analysis of heterozygous *adl1C-1* indicates that the mutation specifically affects post-meiotic male gametogenesis. Fifty percent of the mature pollen from heterozygous *adl1C-1* androecia are shriveled and fail to germinate *in vitro*. During microspore maturation, *adl1C-1* pollen grains display defects in the plasma membrane and intine morphology, suggesting that ADL1C is essential for the formation and maintenance of the pollen cell surface and viability during desiccation. Consistent with a role in cell-surface dynamics, immunofluorescence microscopy indicates that ADL1C is localized to the cell plate of dividing somatic cells and to the tip of expanding root hairs. We propose that ADL1C functions in plasma membrane dynamics, and we discuss the role of the ADL1 family in plant growth and development.

Keywords: cell plate, cell wall, intine, membrane recycling, root hair.

Introduction

Male gametogenesis in flowering plants results in the formation of a multicellular pollen grain. This process occurs through a series of intricate steps that have been described at the cytologic level, using light (Heslop-Harrison, 1978; Regan and Moffatt, 1990) and electron microscopy (El-Ghazaly *et al*., 2001; Kuang and Musgrave, 1996; Van Aelst *et al*., 1993), in many species including *Arabidopsis* (Owen and Makaroff, 1995). However, information about the molecular mechanisms underlying pollen development is limited. The developmental process is initiated with the formation of the diploid microsporocyte, which undergoes two rounds of meiosis, resulting in four haploid microspores bound in a tetrad by a callose cell wall (for review, see McCormick, 1993; Twell *et al*., 1998). Dissolution of the callose cell wall by hydrolytic enzymes supplied by the neighboring sporophytic tapetum releases the individual microspores. Subsequently, each microspore matures into a functional gametophyte through a developmental pathway involving two mitotic events. The first mitotic event, pollen mitosis I (PMI), is an asymmetric cell division, which yields a bicellular pollen grain containing two structurally and functionally distinct cells, a vegetative cell (VC) and a smaller generative cell (GC). The larger VC is metabolically and transcriptionally active and functions to support further development of the pollen grain including intine production (Kuang and Musgrave, 1996). In *Arabidopsis* and many other plants, the GC undergoes a second mitotic division, pollen mitosis II (PMII), to form a tricellular pollen grain. The sperm cells and vegetative nucleus remain associated with one another as a 'male germ unit' (MGU) that is postulated to be necessary for efficient fertilization upon pollen germination (Lalanne and Twell, 2002, and references therein). Pollen grain durability is conferred by a wall composed of exine and intine layers (Fahn, 1990). Like other primary plant cell walls, the intine layer is primarily composed of pectin and cellulose. Intine formation requires extensive secretion of Golgi-derived vesicles containing membrane, protein, and cell-wall precursors. In contrast, the outer exine layer is mainly comprised of material derived from the tapetum of the microsporangium.

Recent studies have identified several mutants that specifically affect male gametogenesis (for review, see Twell *et al*., 1998). The mutants exhibit a range of phenotypes including defects in cell-fate determination, nuclear division during PMI and PMII, GC differentiation, MGU organization, and intine deposition (Chen and McCormick, 1996; Fei and Sawhney, 2001; Grini *et al*., 1999; Lalanne and Twell, 2002; Park and Twell, 2001; Park *et al*., 1998). With

the exception of *gemini pollen* (*gem1*; Park and Twell, 2001), none of the other genes identified by defective male gametophytic mutants have been isolated using positional (i.e. map-based) cloning techniques, perhaps as a result of the low penetrance of the mutant phenotypes. The *gem1* mutation affects mitotic cytokinesis events within the microspore (Park and Twell, 2001; Park *et al.*, 1998). Binucleate microspores with ectopic divisional walls are observed, suggesting that cytokinesis and nuclear division are spatially uncoupled during PMI. Recent studies have shown that GEM1 is identical to MOR1 (Twell *et al.*, 2002), an *Arabidopsis* gene encoding a microtubule-associated protein that is essential for cortical microtubule organization (Whittington *et al.*, 2001). GEM1 is thought to be required for phragmoplast microtubule dynamics necessary for asymmetric division and GC formation during PMI.

Recent reverse genetic approaches have also identified genes that are involved in the latter stages of pollen development. AtPTEN1, a dual-specificity protein tyrosine phosphatase (DsPTP) homolog, exhibits tricellular pollen-specific expression and has been shown to dephosphorylate both phosphotyrosine and phosphatidylinositol (PIP3) lipid substrates *in vitro* (Gupta *et al.*, 2002). RNA interference experiments in transgenic *Arabidopsis* revealed that suppression of *AtPTEN1* expression resulted in pollen death following PMII. In addition, recent findings have shown that several members of the *SYP2* and *SYP4* syntaxin gene families, which function in endomembrane transport vesicle fusion, are required for the formation of viable pollen grains (Sanderfoot *et al.*, 2001). However, the specific stage(s) of male gametogenesis that is affected in loss of function of *syp21*, *syp22*, and *syp41* mutants was not determined.

The morphologic and genetic studies described above have demonstrated that pollen development is highly dependent on membrane trafficking and cytoskeleton dynamics. Indeed, assembly and guidance of the hemispherical cell plate around the GC during PMI requires both these processes (Park and Twell, 2001). In addition, vacuole biogenesis and plasma membrane expansion during microspore development and maturation require extensive membrane flow. Here, we show that a member of the *Arabidopsis* dynamin-like protein family, ADL1C, is required for late-stage pollen development. Dynamins, a family of large GTP-binding proteins, defined by conserved GTP binding (GTPase) and GTPase effector domains (GED), have been implicated in numerous membrane-trafficking- and organelle-inheritance-related processes (van der Bliek, 1999). In particular, animal dynamins have been shown to be required for both clathrin-mediated and clathrin-independent endocytosis (McNiven *et al.*, 2000). *adl1C-1* tricellular pollen grains do not survive desiccation, and thus fail to germinate. We provide cytologic evidence that ADL1C is required for the proper assembly and maintenance of the plasma membrane and intine layer during microspore maturation. By immunofluorescence microscopy, we also show that ADL1C is associated with the cell plate in dividing somatic cells and is localized to the distal tip of the elongating root hairs. Analysis of the *adl1C* mutant phenotype and the localization of ADL1C support a role for this plant-specific dynamin-like protein in plasma membrane dynamics during plant cell division and expansion.

Results

Expression profile of the ADL1 *gene family*

Our studies have suggested that the five members of the *Arabidopsis* dynamin-like protein gene family (*ADL1*), *ADL1A–E*, encode proteins with partially overlapping functions (Kang *et al.*, 2001, 2003). RNA gel blot analysis (Figure 1a) was therefore performed to investigate the distribution of *ADL1A–E* mRNA in various organs. The 3′-regions of the *ADL1A–E* cDNAs, which are most divergent from each other, were used as gene-specific probes. Gene-specificity was confirmed by cross-hybridization analysis (Figure 1b). Weak but detectable cross-hybridization was observed between the *ADL1A* and *ADL1B* probes, and the *ADL1D* and *ADL1E* probes, consistent with their limited sequence identity; based upon pair-wise alignment (Smith *et al.*, 1996), the *ADL1A* and *ADL1B* probes, and the *ADL1D* and *ADL1E* probes showed 72.1 and 74.9% sequence identity, respectively. The probes that did not show any detectable cross-hybridization shared less than 60% sequence identity. Nevertheless, the level of cross-hybridization observed between the *ADL1A* and *ADL1B* probes, and the *ADL1D* and *ADL1E* gene-specific probes was below the limit of detection on gel blots of total RNA (Figure 1a). Of the five *ADL1* genes, *ADL1A*, *ADL1C*, and *ADL1E* were found to be expressed at similar levels throughout the plant. Consistent with this result, BLAST searches (Altschul *et al.*, 1997) of the Stanford *Arabidopsis thaliana* database (http://www.arabidopsis.org/) identified expressed sequence tags (ESTs) corresponding to *ADL1A*, *ADL1C*, and *ADL1E*. Higher levels of *ADL1A*, *ADL1C*, and *ADL1E* mRNA expressions were observed in actively dividing and expanding *Arabidopsis* suspension-cultured cells (T87). Weak but reproducible expression of *ADL1B* and *ADL1D* mRNA was also observed in the T87 cells by RNA blot analysis, and this was confirmed by reverse transcriptase PCR and nucleotide sequencing. Homozygous *adl1B::T-DNA* and *adl1D::T-DNA* insertion mutants, however, did not display any detectable phenotype (data not shown), possibly reflecting the low abundance of the two isoforms and/or functional redundancy. Full-length cDNA sequences for *ADL1B–E* have been deposited in the GenBank database (Accession nos.: *ADL1B*, AY189279; *ADL1C*, AF488808; *ADL1D*, AF488807; *ADL1E*, AF488725).

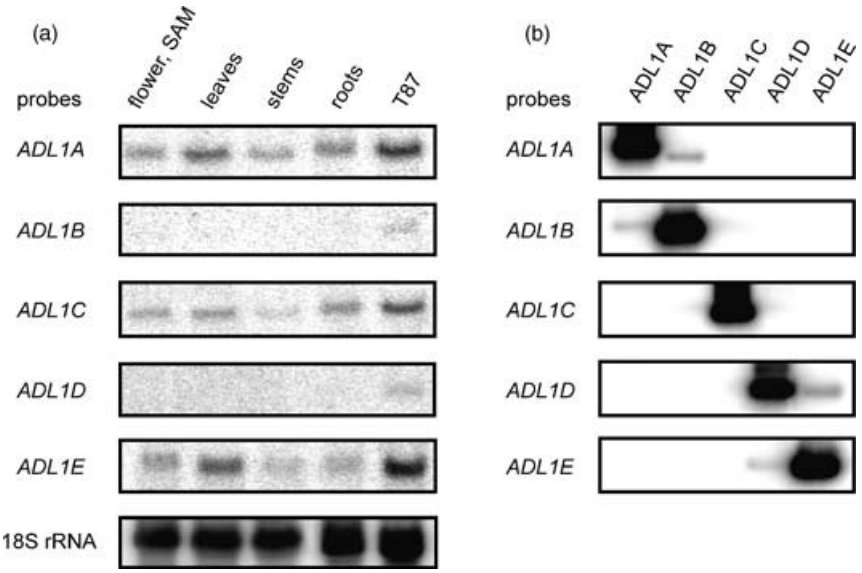

Figure 1. Nucleic acid gel blot analysis of the tissue-specific expression of *adl1* gene family members.
(a) Total RNA was isolated from *Arabidopsis* plants and actively dividing suspension-cultured cells (T87) and probed with *ADL1A–E* gene-specific probes. Blots were hybridized with an 18S rRNA probe as a control for equal loading.
(b) The specificity of the probes was tested by cross-hybridization analysis. Each probe was hybridized to 20 ng unlabeled *ADL1A–E* cDNA used for the synthesis of the ^{32}P-labeled gene-specific probes.

Histochemical localization of ADL1C *promoter activity*

To further examine the tissue-specific and developmental expression profile of *ADL1C*, we generated transgenic lines containing an *ADL1C* promoter bacterial *uidA* β-glucuronidase (GUS) translational fusion construct, *ADL1C-GUS* (Figure 2a). The *ADL1C* promoter utilized in the *ADL1C-GUS* reporter construct was sufficient to control the expression of *ADL1C* for molecular complementation of the *adl1C-1* loss-of-function mutant (see below). Progeny from eight independent transgenic T_2 *ADL1C-GUS* plant lines were used for histochemical localization of GUS enzyme activity. Subtle differences were observed in signal intensity between the individual lines; however, no differences in the tissue and developmental profile of GUS staining were observed. Untransformed and transgenic lines, harboring GUS without the 5′-flanking sequence of *ADL1C*, did not show any GUS activity under the staining conditions employed in this study (data not shown).

The expression profile of the *ADL1C* promoter-GUS fusion construct was significantly different from *ADL1A* and *ADL1E* (Kang *et al*., 2003). GUS staining was observed in emerging leaf primordia and stipules (Figure 2b). In expanding leaves, *ADL1C-GUS* expression was highest near the leaf base, where the cells continued to divide during leaf blade development (Donnelly *et al*., 1999; Figure 2b). No GUS activity was observed in expanding *ADL1C-GUS* leaf trichomes and surrounding socket cells in contrast to *ADL1A* and *ADL1E* (Kang *et al*., 2003). In the roots of *ADL1C-GUS* seedlings, strong GUS staining was observed in the lateral and columella root cap cells, in epidermal trichoblast root cell files of the elongation zone (Figure 2c), and in emerging lateral root primordia with its associated vascular tissue (Figure 2d). Expanding root hairs, which bud from the root-apex end of the outer cell wall of trichoblasts, displayed strong GUS staining (Figure 2e). Weak but detectable GUS activity was also observed in the epidermis of the root transition zone (also known as the distal elongation zone) and in the atrichoblast cell files (Figure 2c).

Strong GUS activity was observed in developing anthers as well as mature pollen grains of *ADL1C-GUS* plants. In young flowers (stage 11; Smyth *et al*., 1990), GUS activity was observed throughout the anthers (Figure 2f). However, *ADL1C-GUS* expression was restricted to developing pollen grains at later stages of flower development (Figure 2g). Pollen-grain-specific GUS expression was observed only after the microspore release from the tetrads (Figure 2h,i), suggesting that *ADL1C* is specifically expressed during post-meiotic pollen development. In addition, *ADL1C-GUS* expression was detected in unexpanded (Figure 2f), but neither in expanding nor in mature stigmatic papillae cells (Figure 2g), as observed for *ADL1A* (Kang *et al*., 2003).

Characterization of affinity-purified ADL1C-specific antibodies

The ADL1A GTPase domain shares 77 and 79% amino acid identity with ADL1E and ADL1C, respectively. Therefore, it is surprising that the ADL1A GTPase domain-specific antisera (α-GTPase) detects a doublet comprised of the 68-kDa ADL1A and 70-kDa ADL1E proteins (Figure 3a,b), but not the 68-kDa ADL1C polypeptide on immunoblots of total leaf protein extracts (Figure 3a; Kang *et al*., 2001, 2003). Quantitative immunoblotting of purified *Escherichia coli*-expressed ADL1C and ADL1E confirmed that the ADL1A α-GTPase had approximately ninefold higher avidity for ADL1E than ADL1C (see Experimental procedures). To examine the subcellular localization of ADL1C, we generated antibodies against the ADL1C-specific peptide,

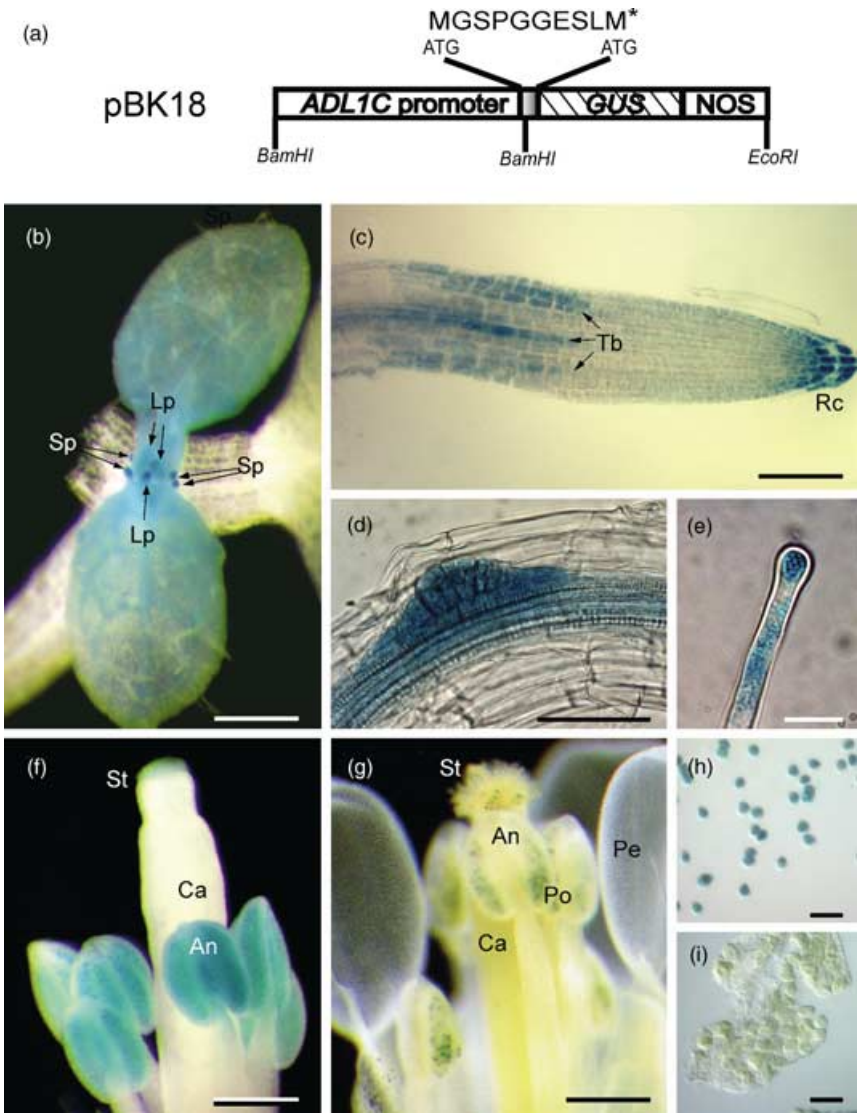

Figure 2. Histochemical localization of *ADL1C-GUS* reporter gene expression.
(a) Schematic diagram of the *ADL1C* promoter-*GUS* translational fusion reporter construct. The deduced 8 amino acid linker between the first amino acid of ADL1C (M) and the GUS start Met (M*) is shown.
(b–i). Analysis of T_2 *Arabidopsis* Wassilewskija (Ws) plants expressing *ADL1C-GUS*. Flower developmental stages are as described by Smyth *et al.* (1990). (b) Shoot apex and emerging primary leaves of a 7-day-old seedling. (c) Root tip and elongation zone of a 5-day-old seedling. (d) Lateral root primordium of a 7-day-old seedling. (e) Growing root hair from a 5-day-old seedling. (f) Unopened flower (stage 11). Petals and sepals were removed prior to imaging. (g) Mature flower (stage 15). (h) Tetrad stage. (i) Released microspores. Anthers containing the microspores in (h) and tetrads in (i) were collected from the same inflorescence.
An, Anther; Ca, Carpel; Ez, elongation zone; Lp, leaf primordium; Pe, petal; Po, Pollen; Rc, root cap cells; Sp, stipules; St, Stigma; Tb, trichoblast cell files; Tz, transition zone. Scale bars are 200 μm in (b–d), 1 mm in (f) and (g), 20 μm in (e), and 40 μm in (h) and (i).

NH_2-EPEKEKPNPRNAPAPNC-COOH (amino acids 496–511; Kang *et al.*, 2001). This epitope is specific to ADL1C, and corresponds to the highly variable and hydrophilic amino acid segment that precedes the C-terminal ADL1 protein family GED domain. Previously, we had prepared isoform-specific antibodies to the equivalent region of the ADL1A protein (Kang *et al.*, 2001). As shown in Figure 3(b), affinity-purified ADL1C-specific antibodies (α-ADL1C) detected a single 68 kDa polypeptide on immunoblots of total leaf protein extracts. Immunoblot analysis of *E. coli*-expressed protein demonstrated reactivity to ADL1C but not to ADL1E (data not shown). Because we were unable to isolate homozygous *adl1C* mutants (see below), α-ADL1C specificity was confirmed by peptide competition analysis. Binding of α-ADL1C to the 68 kDa polypeptide was blocked by excess ADL1C-specific peptide (Figure 3b, lane 2). Equal protein loading was confirmed by Ponceau S staining prior to immunoblot development (data not shown).

Immunolocalization of ADL1C

We examined the localization of ADL1C in actively dividing *Arabidopsis* T87 suspension-cultured cells (Axelos *et al.*, 1992) and in *Arabidopsis* roots by indirect immunofluorescence microscopy using affinity-purified α-ADL1C. Previous studies have demonstrated that ADL1A and ADL1E are associated with the cell plate in dividing *Arabidopsis* cells (Kang *et al.*, 2001, 2003; Lauber *et al.*, 1997). Similarly, strong α-ADL1C immunostaining of the division plane was observed in dividing T87 (red) (Figure 4a) and root cells (green) (Figure 4c). Immunolabeling of the cell plate was blocked in the presence of the ADL1C-specific peptide, confirming the specificity of α-ADL1C labeling of the cell plate (Figure 4b). In addition to the cell plate, ADL1C was found to be associated with punctate intracellular structures in both dividing and non-dividing cells (Figure 4a,c). These structures were similar to ADL1A-positive punctate

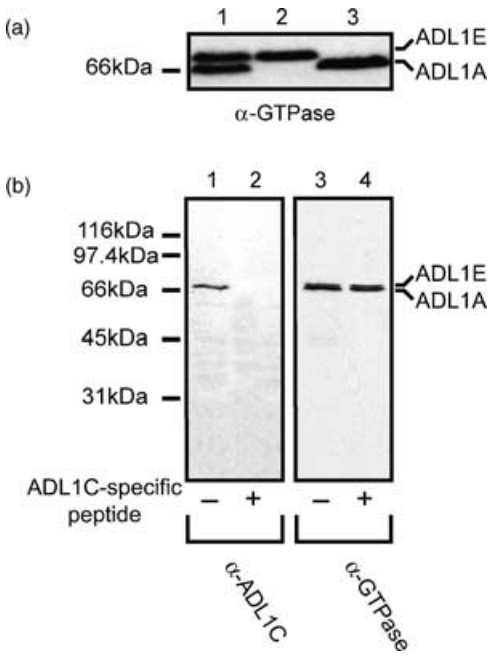

Figure 3. Characterization of affinity-purified ADL1C-specific antibodies (α-ADL1C).
(a) Protein extracts prepared from leaves of *ADL1A/adl1A-2* (lane 1), *adl1A-2/adl1A-2* (lane 2), and *adl1E/adl1E* (lane 3) plants were analyzed by immunoblotting with ADL1 α-GTPase antibodies (Kang *et al.*, 2001). Note that homozygous *adl1A-2* (lane 2) and *adl1E* (lane 3) plant extracts lack the 68 and 70 kDa bands, respectively.
(b) 10 μg of total leaf protein from wild-type *Arabidopsis* plants was analyzed by immunoblotting with α-ADL1C in the absence (lane 1) and presence (lane 2) of the ADL1C peptide antigen. As reported previously, α-GTPase detected the ADL1A/ADL1E (68/70 kDa) doublet (Kang *et al.*, 2001; lane 3). ADL1C-specific peptide does not block binding of α-GTPase to the ADL1A/ADL1E doublet (lane 4).

structures that form as a result of chemical fixation and likely represent aggregates of the normally diffused ADL1-containing intracellular membranes observed in the living cells (Kang *et al.*, 2003).

Immunolocalization studies in wild-type seedling roots revealed that ADL1C is highly expressed in the epidermis of the root elongation zone. Consistent with the expression profile of the *ADL1C-GUS* promoter fusion reporter (Figure 2c), higher levels of ADL1C-specific fluorescence were observed in the epidermal trichoblast versus atrichoblast cell files (Figure 4d,e). ADL1C accumulated at the site of budding root hairs (Figure 4d) and was concentrated in the apical plasma membrane and cytoplasm of the expanding root hairs (Figure 4e,f). No α-ADL1C signal was observed in mature root hair cells or in older root cells above the elongation zone.

Isolation of an adl1C *loss-of-function mutant*

To determine the genomic structure and organization of *ADL1C*, we cloned and sequenced an approximately 2.1-kb cDNA (GenBank accession no. AF488808). Comparison of the *ADL1C* cDNA sequence and its corresponding chromosome I locus, At1g14830, revealed that the genomic copy of *ADL1C* contains 16 exons and 15 introns (Figure 5a). To investigate the biological function of ADL1C, we identified an *adl1C::T-DNA* insertion line, *adl1C-1*, containing a pSKI015 T-DNA insertion in the 13th exon (Figure 5a), upstream of the sequences encoding the critical dynamin GED of ADL1C. PCR genotype analysis of the progeny from self-fertilized heterozygous *adl1C-1* plants showed that they segregated approximately in the ratio of 1 : 1 for heterozygous plants containing the *adl1C-1* mutation and for homozygous wild-type plants (52 heterozygotes:50 wild type). Similarly, heterozygous *adl1C-1* plants exhibited a 1 : 1 segregation ratio (resistant:sensitive) for the pSKI015 T-DNA Bar, ammonium glufosinate (BASTA), resistance marker. No homozygous *adl1C-1* plants were identified, suggesting that *ADL1C* is an essential gene required for gametogenesis (Howden *et al.*, 1998).

adl1C-1 *disrupts post-meiotic pollen development*

No differences in seed set between wild-type and self-pollinated heterozygous *adl1C-1* mutants were observed (>40 seeds per silique), indicating that the *adl1C-1* mutation does not affect female gametogenesis. This was confirmed by PCR genotyping of the progeny from four independent reciprocal crosses between heterozygous *adl1C-1* and wild-type (Wassilewskija (Ws) ecotype) plants. Pollen grains from the wild-type plants were able to successfully fertilize *adl1C-1* plants and yielded plants that segregated in the ratio of 1 : 1 for the T-DNA insertion in *ADL1C* (15 heterozygotes:15 wild type). Conversely, only homozygous *ADL1C/ADL1C* wild-type plants (0 heterozygotes:30 wild type) were recovered when the wild-type plants were pollinated with pollen grains from heterozygous *adl1C-1* flowers. These results indicated that the *adl1C-1* mutation affects male gametophytic development, is fully penetrant, and is thus, not transmitted through the male parent.

Morphologic characterization of mature pollen grains from *adl1C-1* heterozygous plants showed that approximately 50% of them were shriveled (694 normal:680 shriveled; Figure 5b). *In vitro*, the shriveled pollen grains failed to germinate under conditions that permitted successful pollen tube germination and elongation (Li *et al.*, 1999). More than 90% of the pollen grains from the wild-type plants (Figure 5c) and the non-shriveled pollen grains from the heterozygous *adl1C-1* plants (Figure 5d) germinated, whereas the shriveled pollen grains were completely inviable.

To demonstrate that the observed pollen-defective phenotype of heterozygous *adl1C-1* plants was specific to a disruption of *ADL1C,* heterozygous *adl1C-1* plants were transformed with a genomic copy of *ADL1C*. The *ADL1C* transgene (*pBK03K*) includes the entire coding region

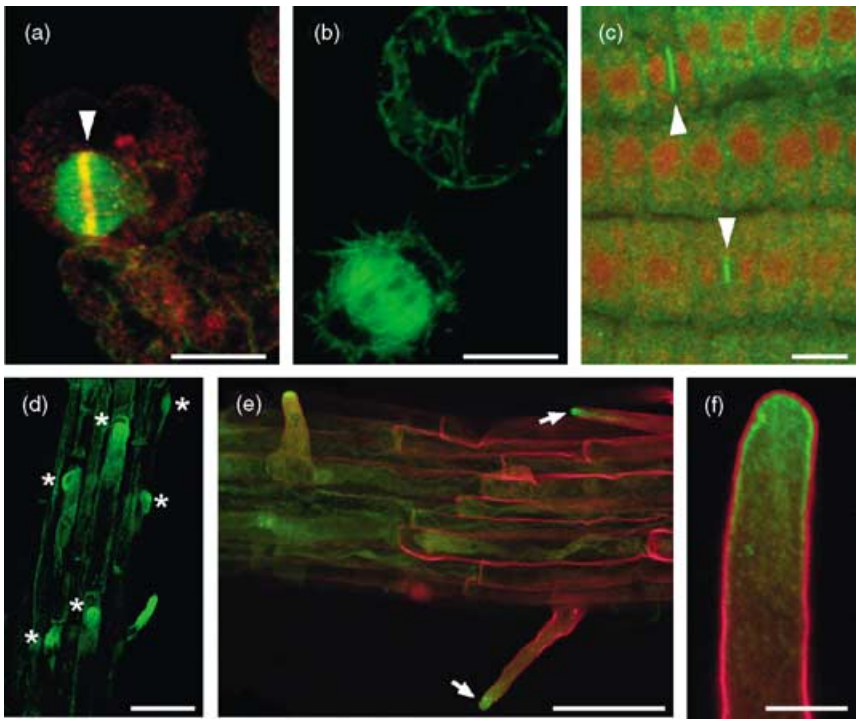

Figure 4. Localization of ADL1C at the cell plate during somatic cell cytokinesis and in the tip of growing root hairs.
(a, b) Protoplasts from a 3-day-old *Arabidopsis* suspension cell-culture were double-immunolabeled with affinity-purified α-ADL1C (red) and α-tubulin to visualize microtubules (green) in the (a) absence and (b) presence of the ADL1C-specific peptide antigen. Cell plate-associated ADL1C (arrowhead) and phragmoplast mictrotubules co-localize (yellow/orange) at the division plane. Scale bars are 10 μm in (a) and (b).
(c) Dividing and interphase root transition zone cells immunolabeled with α-ADL1C (green). Nuclei were stained with propidium iodide (red). Arrowhead denotes cell plate localization of ADL1C. Scale bar is 10 μm.
(d–f) ADL1C is localized to the tip of expanding root hairs. (d) Root epidermal cells displaying ADL1C concentration at the bulges (asterisk) in trichoblasts. (e) ADL1C is localized in the apical tip of expanding root hairs (arrows). (f) Higher magnification view of ADL1C localization in elongating root hairs. The cell wall was stained with propidium iodide (red) prior to fixation (e, f). Scale bars are 50 μm in (d) and (e) and 5 μm in (f).

of *ADL1C*, 1.8 kb of 5′-putative promoter DNA and 2.7 kb of 3′-flanking untranslated DNA. In contrast to heterozygous *adl1C-1* plants, segregation of the wild-type and the mutant pollen grains from eight independent *ADL1C*/*adl1C-1::pBK03K* lines (T_1 generation) deviated significantly from the ratio 1 : 1 (Figure 5e) as a result of independent inheritance of the rescue construct and the *adl1C-1* mutation. The percentage of shriveled pollen grains ranged from 6.25 to 29% of a total number of approximately 400 pollen grains analyzed from each of the eight independent transgenic lines. In addition, we were able to isolate homozygous *adl1C-1* mutant plants containing pBK03K in the T_2 generation (Figure 5f), confirming that the *ADL1C* transgene can complement the *adl1C-1* mutation.

Analysis of pollen development in adl1C-1 *mutants*

To determine when *adl1C-1* pollen grain development deviates from the wild type, we examined various stages of microsporogenesis and microgametogenesis in *adl1C-1* flowers by differential interference contrast (DIC) microscopy and epifluorescence microscopy, after staining with 4,6-diamidino-2-phenylindole (DAPI) to monitor nuclear DNA content. No defects in microsporogenesis, including tetrad formation, and microspore release were observed (Figure 6a,b,d,e). The tetrads from heterozygous *adl1C-1* plants consisted of four identical microspores. After microspore release, all the pollen grains underwent normal nuclear migration to form polarized microspores (Figure 6c,f). Following PMI, all pollen grains contained a VC and a GC nucleus (Figure 6g,j), and no defects in GC migration and PMII were observed (Figure 6h,k). Just prior to anthesis (stage 12–13 flowers), when pollen grains undergo desiccation (Smyth *et al.*, 1990), we detected pollen grains lacking DAPI-stained nuclear material (Figure 6i,l). The pollen grains lacking nuclear staining collapsed during desiccation, resulting in the shriveled pollen grains.

Defects in the adl1C-1 *pollen grain cell wall and plasma membrane*

To further compare the development and maturation of wild-type and *adl1C-1* pollen, we utilized thin section transmission electron microscopy (TEM) to examine the

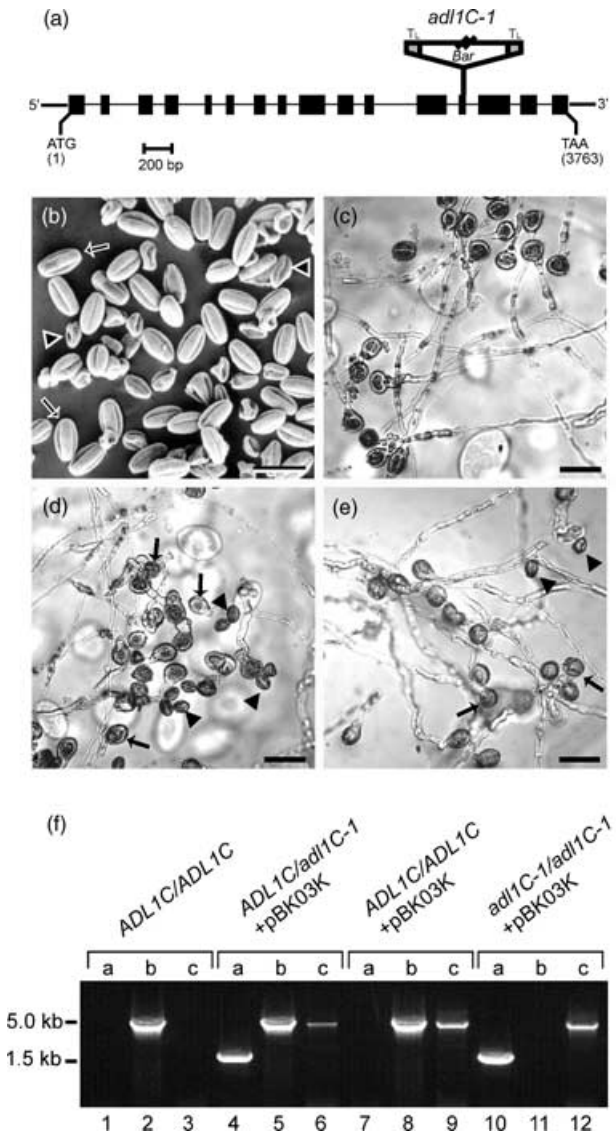

Figure 5. Identification and molecular complementation of *adl1C-1* pollen.
(a) Schematic diagram of the exon/intron structure of *ADL1C*. Boxes and lines represent exons and introns, respectively. The position of the T-DNA insertion is indicated with a triangle. ATG and TAA signify the positions of the translation, initiation, and termination codons. Exons and introns are drawn to scale (bar = 200 bp), but the T-DNA is not. *Bar*, glufosinate-resistance T-DNA selection marker gene; T_L, T-DNA left border.
(b) Scanning electron micrograph of mature normal (arrows) and shriveled pollen (arrowheads) grains shed from *adl1C-1* flowers.
(c–e) *In vitro* pollen tube germination assay. Pollen grains from (c) wild-type, (d) heterozygous *adl1C-1*, and (e) heterozygous *adl1C-1*::*pBK03K* (T_1 generation) were assayed. Arrowheads and arrows indicate shriveled and normal pollen grains, respectively. Scale bars are 40 μm in (b–e).
(f) Molecular analysis of rescued *adl1C-1* plants. Ethidium-bromide-stained agarose gel of PCR-amplified genomic DNA products from untransformed wild type (lanes 1–3), heterozygous *adl1C-1/ADL1C*::pBK03K (lanes 4–6), wild-type transformed with pBK03K (lanes 7–9), and T_2 homozygous *adl1C-1*::pBK03K (lanes 10–12) plants. Oligonucleotide primer pairs specific for *adl1C-1*::*T-DNA* (1.5 kb), *ADL1C* and the rescue construct (5 kb), and pBK03K (5 kb) were used to distinguish wild-type, heterozygous, and rescued homozygous *adl1C-1* mutants.

ultrastructure of developing wild-type and mutant pollen grains following PMI. As early as the bicellular stage, approximately 50% of the pollen grains displayed irregular plasma membrane morphology (Figure 7a,b). Consistent with their role in GC and pollen cell wall (intine) formation (Kuang and Musgrave, 1996), numerous Golgi stacks and secretory vesicles were observed in the VC cytoplasm of the wild-type (data not shown) and defective (Figure 7b) pollen grains, suggesting that exocytosis was unaffected in the mutants. No other morphologic defects in the GC and VC organelles including lipid bodies, plastids, mitochondria, and endoplasmic reticulum were observed in the mutant pollen grains prior to desiccation. The double membrane that encloses the GC appeared morphologically normal in the mutant pollen grains. The elaboration and infolding of the plasma membrane became more severe at the tricellular stage of development in the *adl1C-1* mutant pollen grains (Figure 7c,d). When compared with the wild-type pollen grains (Figure 7e), the cell wall of the mutant pollen grains (Figure 7d) was less electron-dense and devoid of channel-like structures. In contrast to the wild type (Figure 7h,i), the mutant pollen grains collapsed during desiccation, concomitant with organelle disruption (Figure 7f,g). Occasional separation of the defective pollen cell wall from the mutant pollen grain exine surface was observed (Figure 7g, arrow). No differences in the morphology of the exine layer, which is derived from the tapetal cells of the maternal pollen sac, were observed in the wild-type and the mutant pollen grains.

Discussion

Dynamins have been shown to function in both clathrin-mediated as well as non-clathrin-dependent endocytic processes in animal cells (McNiven *et al.*, 2000). Recent studies suggest that both mechanisms may be involved in the removal of excess plasma membrane in plants. Clathrin-coated vesicles have long been shown to form at the plasma membrane in a wide variety of plant cells (for review, see Battey *et al.*, 1999; Holstein, 2002). More recent electrophysiologic and morphometric studies have suggested that plant endocytosis may also involve the internalization of vesicles, significantly larger than the clathrin-coated vesicles (Homann and Thiel, 1999; Kubitscheck *et al.*, 2000). Generation of these vesicles may be similar to the clathrin-independent formation of large invaginations involved in yeast plasma membrane endocytosis (Mulholland *et al.*, 1994, 1999).

Common phenotypes observed in the mutant cells lacking one or more members of the plant-specific *ADL1* dynamin-like protein family are plasma membrane proliferation and aberrant cell wall structure. Here, we show that ADL1C is essential for the formation of viable pollen grains. Expression of *ADL1C* correlates with the time of

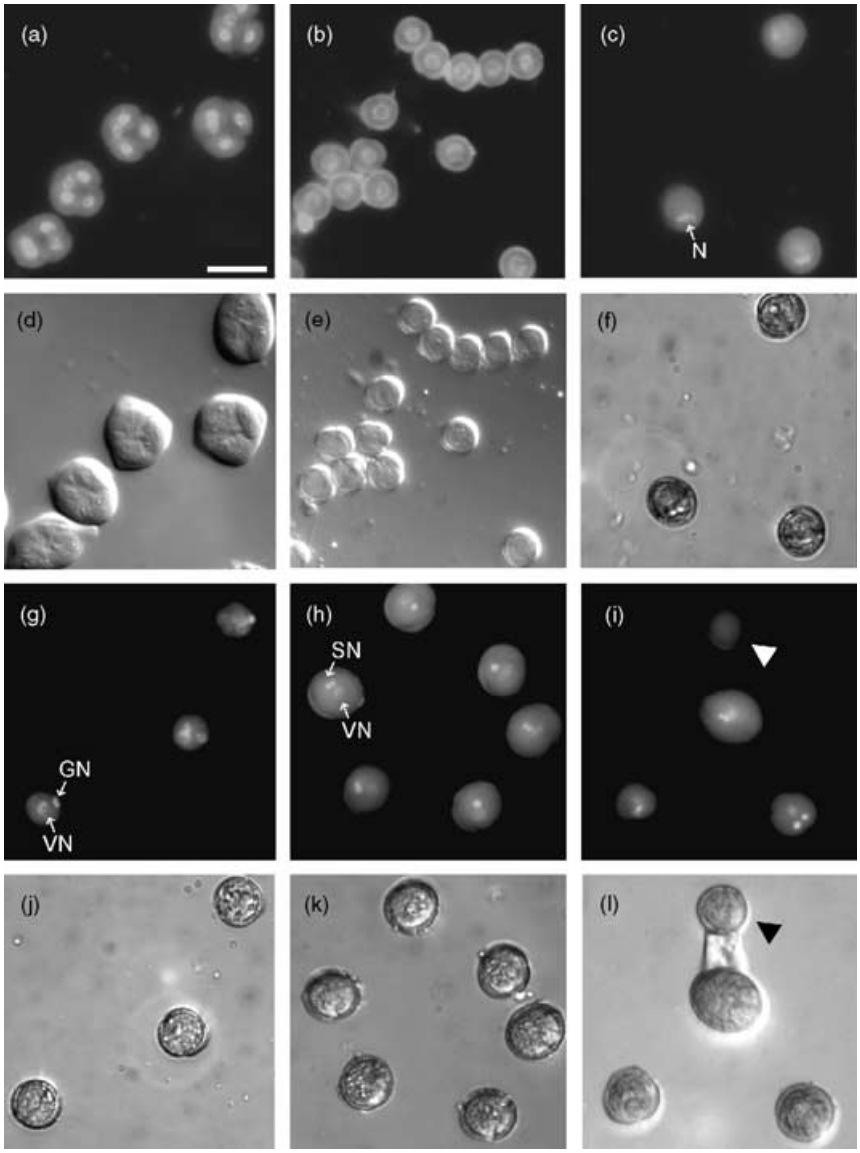

Figure 6. Cytochemical analysis of *adl1C-1* mutant pollen development.
Pollen grains were examined by epifluorescence microscopy after 4,6-diamidino-2-phenylindole (DAPI) staining (a–c, g–i) and differential interference contrast (DIC) optics (d–f, j–l). (a, d) Tetrad stage. (b, e) Microspores released from tetrads. (c, f) Vacuolate stage. (g, j) Bicellular stage. (l, l) Onset of desiccation. Note a pollen grain (arrowhead) lacking nuclei (l). GN, generative nucleus; N, microspore nucleus; SN, sperm nuclei; VN, vegetative nucleus. Scale bars are 20 μm in (a–l).

post-meiotic microspore expansion. Ultrastructural analysis of developing *adl1C* mutant pollen grains suggests that the defective pollen grains are desiccation-intolerant, possibly as a result of defects in plasma membrane maintenance and intine formation. We have observed similar plasma membrane/cell wall defects in other cells, but not in the pollen of *adl1A* and embryo-lethal *adl1A*; *adl1E* double mutants (Kang *et al.*, 2003). As *adl1A* stigmatic papillae cells expand, there is a dramatic accumulation of plasma membrane, accompanied by a progressive loss of cell wall material. In rapidly expanding cells, it has been estimated that more than 75% of the total membrane delivered to the plasma membrane, via fusion of exocytic vesicles, is recycled (Battey *et al.*, 1999; Samuels and Bisalputra, 1990). A block in endocytosis therefore would be predicted to lead to the accumulation of plasma membrane by uncoupling the exocytic/endocytic membrane flow cycle. Perhaps, failure to endocytose and/or localize hydrolytic enzymes involved in cell wall biosynthesis and modification, such as the plasma-membrane-associated endo-1,4-β-D-glucanase KORRIGAN (Nicol *et al.*, 1998), could lead to the abnormal cell wall structure. KORRIGAN is required for the synthesis of cellulose (Sato *et al.*, 2001), a major constituent of the pollen grain intine layer (Regan and Moffatt, 1990).

In addition to the well-established role of dynamins in plasma membrane internalization (Sever *et al.*, 1999), dynamins and dynamin-related proteins are involved in many other cellular processes such as peroxisome biogenesis (Hoepfner *et al.*, 2001; Koch *et al.*, 2003), mitochondria maintenance (Arimura and Tsutsumi, 2002; Wong *et al.*, 2000), chloroplast division (Miyagishima *et al.*, 2003), and

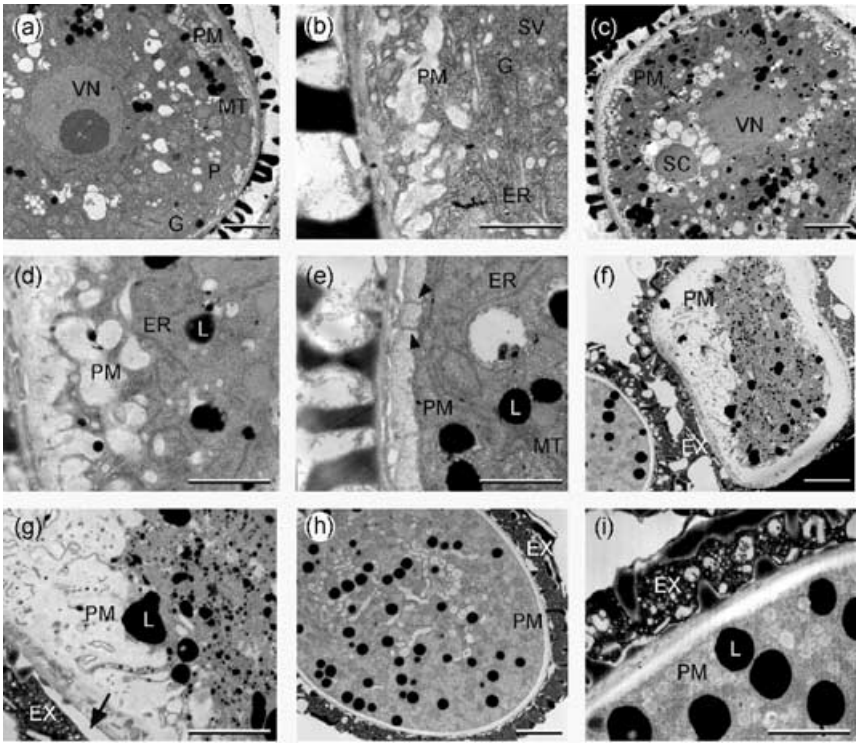

Figure 7. Transmission electron microscopy (TEM) analysis of *adl1C-1* mutant and wild-type pollen grains.
(a) *adl1C-1* mutant pollen grain at the bicellular stage.
(b) High magnification view of the cortical region of the *adl1C-1* mutant pollen grain at the bicellular stage.
(c) *adl1C-1* mutant pollen grain at the tricellular stage.
(d) High magnification view of the plasma membrane of a tricellular *adl1C-1* mutant pollen grain.
(e) High magnification view of the cell surface of a wild-type pollen grain. Channel-like structures are marked with arrowheads.
(f) *adl1C-1* mutant pollen grain during desiccation.
(g) High magnification view of the cortex of a collapsing *adl1C-1* mutant pollen grain. Arrow indicates separation between exine layer and pollen cell wall.
(h) Mature wild-type pollen grain.
(i) High magnification view of a mature wild-type pollen grain.
ER, endoplasmic reticulum; EX, exine layer; G, Golgi apparatus; L, lipid body; MT, mitochondria; P, plastid; PM, plasma membrane; SC, sperm cell; VN, vegetative nucleus. Scale bars are 2 μm in (a), (c), (f), and (h) and 1 μm in (b), (d), (e), (g), and (i).

actin cytoskeleton dynamics (Orth and McNiven, 2003). In mammalian cells, dynamin interaction with the actin cytoskeleton has been shown to regulate membrane protrusion, tubulation, as well as endocytosis (Lee and De Camilli, 2002; Ochoa *et al.*, 2000; Orth *et al.*, 2002). Functional links between dynamins and the actin cytoskeleton are thus particularly interesting in view of the plasma membrane proliferation in *adl1C-1* pollen grains and the localization of ADL1C at the tip of the growing root hairs. Endocytosis in yeast and mammalian cells involves remodeling of cortical actin cytoskeleton (Schafer, 2002). Similarly, disruption of filamentous actin affects the internalization of cell wall material in root cells (Baluska *et al.*, 2002). The actin cytoskeleton at the tip of the expanding root hairs is dynamic, and has been proposed to regulate exocytosis and endocytosis (Ketelaar *et al.*, 2003). Therefore, defective actin dynamics could lead to failure in the plasma membrane maintenance and cell wall formation in certain types of plant cells.

For pollen, proper formation of the intine layer has been shown to be critical for survival during desiccation (Fei and Sawhney, 2001; Grini *et al.*, 1999). We propose that the abnormal architecture of the intine and plasma membrane results in the collapse and death of the *adl1C-1* mutant pollen grain. Whereas the *adl1C-1* phenotype is restricted to male gametogenesis, expression and localization studies suggest that ADL1C may function in other tissues and stages of plant growth and development.

ADL1C is localized at the tip of growing root hairs

Our results suggest a general role for ADL1 proteins in polarized cell expansion. Polarized plant cell expansion is achieved through two distinct but inter-related processes, tip growth and diffuse growth (Kropf *et al.*, 1998). Diffuse growth is characterized by dispersed deposition of new plasma membrane and cell wall material across the length of an expanding cell surface. In tip growth, targeting and

fusion of Golgi-derived exocytic vesicles are highly polarized toward the apical dome of the expanding cells. In higher plants, only the root hairs and the pollen tubes have been shown to rely on tip growth for their development. Root hairs grow in phases: first, a bulge forms on the basal end of the epidermal root trichoblast cells, which then elongates by polarized growth. We have shown that *ADL1C* was highly expressed in trichoblast cell files and during root-hair budding. Consistent with this, ADL1C protein was concentrated at the site of root-hair emergence. In the expanding root hairs, ADL1C was predominantly associated with the apical plasma membrane and subcortical cytoplasm at the tip of the hairs. As shown in tip-growing pollen tubes, the exocytic flow of membrane and cell wall material to the root hair tip is likely to be balanced by equally active endocytosis (Battey *et al.*, 1999; Hepler *et al.*, 2001). Indeed, ultrastructural analysis of growing *Arabidopsis* root hairs has shown the presence of numerous coated and non-coated vesicles near the apical plasma membrane of the expanding hairs, which may constitute membrane recycling (Galway *et al.*, 1997). Based on its localization in root hair tips, we hypothesize that ADL1C may be required directly or indirectly in plasma membrane recycling during growth of the root hair tip. In addition to root hairs, our expression and localization studies have demonstrated that ADL1C is expressed in cells that expand via diffused growth. Therefore, it is likely that ADL1C-mediated PM dynamics may also be required for diffuse cell expansion as shown for ADL1A and ADL1E (Kang *et al.*, 2003).

In addition to its role in cell expansion, ADL1C is likely to be required for construction of the cell plate during plant cytokinesis, which also involves polarized membrane trafficking and recycling (Bednarek and Falbel, 2002). ADL1C was found to be expressed in actively dividing suspension-cultured cells and in regions of the leaf and root which contain actively dividing cells including emerging leaf primordia, the base of expanding leaves, emerging lateral root initials, and in cells of the root transition zone. Similar to ADL1A and ADL1E (Kang *et al.*, 2001, 2003), we have shown that ADL1C is associated with the cell plate in dividing suspension-cultured cells and root cells. Analysis of embryo-lethal *adl1A*; *adl1E* double mutants has demonstrated that ADL1A and ADL1E are required for cell plate membrane consolidation and maturation during embryogenesis (Kang *et al.*, 2003). In contrast, no defects in the formation of the hemispherical cell plate that forms around the GC during PMI were observed in *adl1C-1*. One possible explanation for this is that assembly of the unique architecture of the pollen cell plate (Park and Twell, 2001) does not require ADL1C-mediated membrane recycling.

Isotropic microspore expansion was not affected by the *adl1C-1* mutation. Wild-type and *adl1C-1* pollen grains were of the same size prior to desiccation (Figure 6). Interestingly, *adl1A* mutant stigmatic papillae, which normally undergo anisotropic expansion to form flask-shaped cells, were observed to expand isotropically (Kang *et al.*, 2003). Therefore, our results suggest that ADL1-mediated membrane dynamics is required for polarized, but not isotropic, cell growth.

Pollen development, a polar molecular process?

The molecular mechanisms of pollen grain maturation are not fully understood. Pollen maturation involves expansion of the microsporocyte coupled to vacuole-mediated nuclear migration, resulting in a polarized cell that goes through asymmetric division during PMI. A continued intrinsic polarization of the developing pollen grain must be maintained in order to establish a site of exit for pollen-tube emergence upon germination. In the latter case, the establishment and maintenance of those sites may require biochemically distinct plasma membrane domains to be established prior to desiccation. With *adl1C-1* pollen, we observed no difference in the size when compared to the wild-type pollen grains prior to desiccation. These results suggest that microspore exocytosis and expansion were not affected by the *adl1C-1* mutation. Plasma membrane proliferation, which is also observed in other *adl1* mutant cells, was first observed in bicellular *adl1C-1* pollen grains, and it continued throughout the later stages of pollen development. It is intriguing to speculate that the latter stages of pollen development, prior to desiccation, require the establishment of polarized plasma membrane domains that are crucial for pollen survival and viability. This process may be dependent upon ADL1C-mediated plasma membrane maintenance. Interestingly, AtPTEN1, a putative tyrosine phosphatase required for pollen maturation, has been shown to convert phosphatidylinositol triphosphate (PIP3) to phosphatidylinositol bisphosphate (PIP2; Gupta *et al.*, 2002), a potent activator of various plant and animal dynamins and dynamin-like proteins (Achiriloaie *et al.*, 1999; Kim *et al.*, 2001; Lam *et al.*, 2002; Lin *et al.*, 1997; Zheng *et al.*, 1996). AtPTEN1 function may therefore be required for ADL1C-mediated PM dynamics during pollen maturation.

Pollen development and beyond, a role for ADL1C*?*

ADL1C, *ADL1A*, and *ADL1E* show both overlapping and unique tissue-specific and cell-type-specific expression patterns in developing *Arabidopsis*, suggesting distinct developmental functions. Consistent with this hypothesis, *adl1A* and *adl1C* mutants display cell-type-specific morphologic phenotypes. Further genetic analysis of ADL1C function during plant growth is hindered by the male inheritance defect of the *adl1C-1* mutation. To study the effects of the *adl1C* loss-of-function mutation on cell plate formation and cell expansion in other cell types, including pollen tube elongation and root hair growth, it will be necessary to

specifically rescue *adl1C-1* pollen development. One approach is to complement the pollen-defective *adl1C-1* phenotype by expressing *ADL1C* under control of a pollen-specific promoter such as the *LAT52* promoter, which regulates the expression of a cysteine-rich extracellular protein (Tang *et al.*, 2002), late in the VC during pollen maturation (Twell *et al.*, 1991). Attempts to rescue *adl1C* pollen development by using a *LAT52* promoter *ADL1C* fusion construct, however, were not successful (data not shown), perhaps because of the differences in the timing and/or level of expression of *ADL1C* and *LAT52* gene products. An alternative approach will be the use of inducible promoter systems to regulate ADL1C expression. Further analysis of ADL1C localization and biochemical characterization of ADL1C and interacting proteins will provide additional insight into the regulatory mechanisms underlying plant cell division and expansion.

Experimental procedures

General

Standard recombinant DNA procedures were carried out as described by Ausubel *et al.* (1989–1995), unless otherwise noted. Enzymes for the manipulation of nucleic acids were purchased from New England Biolabs (Beverly, MA, USA) or Amersham Biosciences Corp. (Piscataway, NJ, USA), unless indicated. All other reagents, unless specified, were from Sigma Chemical Co. (St. Louis, MO, USA).

Plant material and growth conditions

Wild-type and *adl1C-1* mutant plants (*Arabidopsis thaliana* Ws ecotype) were grown on soil (Germination Mix, Conrad Fafarad, Agawam, MA, USA) at 24°C. Plants were fertilized with 2 g l^{-1} Dyna-Grow 7-9-5 fertilizer (Dyna-Grow Corp., San Pablo, CA, USA) once after germination, and were grown under continuous light or long-day conditions (16 h light and 8 h dark). *adl1C-1* mutant plants were selected on soil by spraying (every other day for 1 week) with 20 μg ml^{-1} ammonium glufosinate (Liberty, Wilmington, DE, USA). Transgenic plants transformed with pBK03K and pBK18 were selected on sterile solidified (0.6% phytoagar) MS medium (Murashige and Skoog, 1962; Life Technologies, Rockville, MD, USA) without hormones, and were supplemented with 40 μg ml^{-1} kanamycin. Preparation of total leaf protein extracts for immunoblotting and the characterization of the anti-ADL1A GTPase-specific antibodies are as described by Kang *et al.* (2001). To collect root tissue for total RNA preparation, wild-type seeds were germinated and grown in sterile liquid hormone-free MS medium with gentle shaking (~ 0.035 ***g***) for 6 days at 22°C under continuous illumination. *Arabidopsis* suspension-cultured cells (T87; Axelos *et al.*, 1992) were maintained as described by Kang *et al.* (2001).

Oligonucleotides

All oligonucleotides used in this study were synthesized by Integrated DNA Technologies Inc. (Coralville, IA, USA), and are listed in Table 1. Restriction site sequences used in cloning are shown in lower-case letters.

Table 1 Oligonucleotides used in this study

Name	Sequence (5′→3′)
SB86	GGTGGTAACCCCACACACTCCATTTT
SB87	AACGATACGTAACATATCGGGTGATGGAC
SB88	AGCTTCATGTAGAAAGCCAAAACATGT
SB89	AGATAACCACAAGTACTACAATAGTTGTC
SB90	ATCTTGAACCCGAGAAAGAGAAACCAAAC
SB92	GTTCTCTAAAACCATCACCAGAAACACAC
SB105	CACAGCAAAAACCAAACCGCTTCTCCTTC
SB119	GTGTATGTTTGTGTAGACTGGAAGTTAGA
SB126	GTTCCAGGAAACATGGCGACGATGAAAG
SB127	AGAGAGTCGATATGATTGCTGCACGTAGA
SB206	GGGTTCAAGATGGAGTTTCCTGAACT
SB242	AAATGGAGTGTGAAGAGAGGGTCTCGTCT
SB245	cgggatccTCATAGCTGCGGGACACCATCTT
SB246	cgggatccTTTCATCGTCGCCATGTTTCCTGG
SB256	TTGTGAGCGGATAACAATTTCACACAGGA
SB253	ccggaattcGATGGAGAGTTTGATTGGGTT
SB353	ACTGCTCATTCACCAGATTGAGTATATTCA
SB354	ggaattcCATATGAAAAGTTTGATAGGTCT
SB355	ccgctcgagCTTCCAAGCCACTGCATC
SB357	ccgctcgagTCTTACCCAAGCAACAGATC
SB358	AGGTGGGAATCCGACACATTCGATATTCG
SP6	TACGATTTAGGTGACACTATAG
T7	GTAATACGACTCACTATA
Bar6	GATAGAGCGCCACAATAACAAACAA

Molecular cloning of ADL1 gene family cDNAs

Full-length cDNAs encoding the five ADL1 proteins were synthesized from total RNA of *Arabidopsis* suspension-cultured cells as described previously by Kang *et al.* (2001). Nucleotide sequences of the five cDNAs were determined, and *ADL1B–E* cDNA sequences were deposited in GenBank (Accession nos.: *ADL1B*, AY189279; *ADL1C*, AF488808; *ADL1D*, AF488807; *ADL1E*, AF488725). To generate gene-specific probes for RNA blot analysis, the 3′-regions of *ADL1A–E*, cDNAs (3′-cDNAs) were PCR-amplified with following oligonucleotide pairs using ExTaq (Panvera, Madison, WI, USA) and subcloned into pGEM-T easy vector (Promega, Madison, WI, USA): *ADL1A*, SB86 and SB87; *ADL1B*, SB358 and SB242; *ADL1C*, SB90 and SB119; *ADL1D*, SB88 and SB890; *ADL1E*, SB105 and SB92.

RNA isolation and RNA gel blot analysis

Shoot apical meristems with mature flowers, stems, leaves from mature *Arabidopsis* plants, and root tissue from 6-day-old liquid-cultured seedlings were collected and frozen in liquid nitrogen. Total RNA was prepared with Tri reagent (Sigma, St. Louis, MO, USA), according to the manufacturer's instruction. For RNA gel blots, 15 μg of total RNA was separated by electrophoresis on a 1.2% denaturing formaldehyde agarose gel and was transferred to the Hybond (Amersham Biosciences Corp.) membrane, according to the manufacturer's protocols. Gene-specific probes were prepared using the 3′-regions of *ADL1A–E* cDNAs and labeling with adenosine 5′-[α-^{32}P]triphosphate (triethylammonium salt; Amersham Biosciences Corp.) by the random hexamer method (Ausubel *et al.*, 1989–1995). The RNA blots were hybridized with gene-specific probes at high-stringency conditions (250 mM Na_2HPO_4, 1.0 mM EDTA, 1.0% casein, 7.0% SDS, at 65°C) for 16 h. Following two washes at 65°C in 2× SSC, 0.1% SDS for

30 min, the blots were scanned with a Phosphoimager (Molecular Dynamics, Sunnyvale, CA, USA). To confirm equal loading of RNA, membranes were stripped and re-probed with a ^{32}P-labeled 18S rRNA probe. To test specificity of the probes, 20 ng of purified DNA, which served as templates for radioactively probe synthesis, was blotted to the Hybond membrane and probed as described above.

Isolation of adl1C-1 *and molecular complementation*

The PCR-based identification of *adl1C-1* was performed as described by Kang *et al*. (2001) and Krysan *et al*. (1996). The *ADL1C* T-DNA tagged mutant line was isolated from the pSKI015 BASTA-resistant T-DNA tagged mutant lines available from the University of Wisconsin-Madison Arabidopsis Knockout Facility (http://www.biotech.wisc.edu/Arabidopsis/), using *ADL1C*-specific primers SB119 and SB126, and the T-DNA specific primer Bar6. The *adl1C-1* plants were back-crossed two times to the wild-type WS ecotype. For molecular complementation, a 13.2-kb *Sac*I fragment containing a genomic copy of *ADL1C* was isolated from the IGF clone F10B6 (Mozo *et al*., 1998) and was subcloned into pPZP211 (Hajdukiewicz *et al*., 1994). The resulting vector was further modified to disrupt a second open-reading frame (ORF) included in the *Sac*I fragment by excision of an approximately 3.8-kb *Eco*O109I fragment and religation of the vector. The final complementation vector pBK03K was introduced into the *adl1C-1* heterozygous plants by floral dip transformation method (Clough and Bent, 1998). Homozygous *adl1C-1* plants containing pBK03K were identified by PCR-based genotyping using primers SB127, SB353, SB256, and Bar6. Primer pairs (SB127 + Bar6), (SB127 + SB353), and (SB127 + SB256) were used in separate PCR reactions to amplify *adl1C::T-DNA*, *ADL1C*, and the pBK03K rescue construct, respectively.

Construction of the ADL1C-GUS *fusion construct*

The bacterial *uidA* (GUS) gene and the nopaline synthase (NOS) terminator from pBI121 (Clontech, Palo Alto, CA, USA) were subcloned into the *Eco*RI-*Hin*dIII site of pPZP211, and were designated as pBK08. Using the IGF BAC F10B6 as a template, an approximately 2.0-kb fragment containing the *ADL1C* promoter region was PCR-amplified with SB245 and SB246, and was cloned as a *Bam*HI fragment into pBK08 to generate a translational fusion between the *ADL1C* promoter and the *GUS* coding sequence, pBK18. The 5′-promoter region of *ADL1C-GUS* in pBK18 is 123 bp longer than that of pBK03K, which was used for molecular complementation analysis of *adl1C-1*. The *ADL1C* promoter/*GUS* reporter-gene fusion vector, pBK18, was introduced into the wild-type *Arabidopsis* WS ecotype as described above. T_2 transgenic lines containing pBK18 were used for histochemical staining as described by Kang *et al*. (2003).

Preparation of bacterially expressed recombinant proteins

To generate C-terminal hexahistidine (his_6)-tagged ADL1C and ADL1E bacterial expression plasmids, *ADL1C* and *ADL1E* cDNAs were PCR-amplified (ADL1C, SB354 and SB355; ADL1E, SB253 and SB357), digested with restriction enzymes (*ADL1C*, *Nde*I and *Xho*I; *ADL1E*, *Nco*I and *Xho*I) and subcloned into pET29B (Novagen, Madison, WI, USA). ADL1C- and ADL1E-his_6 fusion proteins were expressed in *E. coli* strain BL21(DE3)LysS and were purified under denaturing conditions on Ni-NTA resin (Qiagen Inc., CA, USA), according to the manufacturer's instructions. To generate the *GST-ADL1C* (amino acids 466–612) expression vector, a 513-bp *ADL1C* PCR product was amplified using the oligonucleotide pair, SB245 and SB246. The PCR product was subcloned as a *Bam*HI fragment into pGEX4T-1 (Amersham Biosciences Corp.), and the resulting vector was designated as pBK09. pBK09 was transformed into the *E. coli* strain BL21(DE3)LysS, and GST-ADL1C (amino acids 466–612) was purified as described by Rancour *et al*. (2002). Protein concentrations were measured with the BioRad Protein Assay kit (BioRad, Richmond, CA, USA), using bovine serum albumin (BSA) as a known standard, and the purity was confirmed by SDS–PAGE followed by staining with Coomassie blue.

ADL1C antibody preparation

To generate ADL1C-specific antibodies, the peptide NH_2-EPE-KEKPNPRNAPAPNC-COOH was synthesized by the UW-Madison Biotechnology Center Peptide Synthesis Facility, coupled to maleimide-activated keyhole limpet hemocyanin (Pierce Chemicals, Rockford, IL, USA) via the C-terminal Cys residue, and used to immunize a rabbit. For affinity purification of rabbit ADL1C-specific antibodies, 1.2 mg GST-ADL1C (466–612) was covalently coupled to 0.5 ml of glutathione sepharose (Amersham Biosciences Corp.), utilizing the cross-linking reagent dimethyl pimelimidate-HCl as described by Bar-Peled and Raikhel (1996), with minor modifications. The coupling reaction was terminated by washing the resin with 30 ml 100 mM Tris–HCl (pH 8.0) and was incubated in 100 mM Tris–HCl (pH 8.0) at 4°C for 12 h. Coupling efficiency was determined by SDS–PAGE as described by Harlow and Lane (1988), and was typically greater than 95%. The resin was equilibrated and stored in Tris buffered saline (TBS), pH 7.4 (25 mM Tris–HCl, pH 7.4, 137 mM NaCl, and 2.7 mM KCl) containing 0.2% (w/v) NaN_3 at 4°C. Rabbit anti-ADL1C antibodies were affinity-purified as described previously by Kang *et al*. (2001).

Immunofluorescence microscopy

Preparation and immunostaining of *Arabidopsis* suspension-cultured cell protoplasts were performed as described by Rancour *et al*. (2002). For whole-mount *Arabidopsis* root indirect immunofluorescence microscopy, the *Arabidopsis* seedlings were grown vertically on solidified (0.6% phytoagar) MS medium (Murashige and Skoog, 1962) under continuous light for 6 days and were processed as described by Kang *et al*. (2003). Cell walls were visualized by incubating live seedlings in 50 mM Piperazine-1,4-bis(2-ethanesulfonic acid) (PIPES), 5 mM EGTA, 5 mM $MgSO_4$ pH 7.0 (MTSB), containing 10 μg ml^{-1} of propidium iodide for 10 min at room temperature (RT), prior to fixation. Nuclear staining was carried out by incubating tissue samples after immunolabeling in PBS containing 10 μg ml^{-1} of propidium iodide for 5 min at RT. For immunolocalization, affinity-purified ADL1C-specific antibodies were diluted in MTSB containing 3% (w/v) BSA (final concentration = 1.4 μg ml^{-1}).

In vitro *pollen germination assay*

Pollen viability and germination was monitored as essentially described by Li *et al*. (1999). Fully open flowers were harvested and allowed to dehydrate at RT for 90 min on the bench. Pollen grains were then transferred to pollen germination media (18% (w/v) sucrose, 0.6% (w/v) phytagar, 0.01% (w/v) boric acid, 1 mM $MgSO_4$, 2.5 mM $CaCl_2$, 2.5 mM $Ca(NO_2)_2$, pH 7.0)) by streaking the dried flower on the surface of the pollen germination medium. Pollens were germinated at 28°C for 6 h and were observed on an Axioskop (Carl Zeiss, Thornwood, NY, USA) with 20× objectives in combination with phase contrast filter sets. Digital images were captured with a cooled charge-coupled device digital camera

containing a 1317 × 1035 pixel array (MicroMax, Princeton Instruments, Trenton, NJ, USA) and processed using IPLab Spectrum (Signal Analytics, Vienna, VA, USA) and Adobe Photoshop (Adobe Systems, San Jose, CA, USA) imaging software on MacIntosh computers (Apple Computer, Cupertino, CA, USA).

Analysis of pollen development

Mature pollen grains were collected by submerging open flowers in 500 μl DAPI staining solution (100 mM sodium phosphate, pH 7.0, 1 mM EDTA, 0.1% (v/v) TX-100, 0.4 μg ml^{-1} DAPI) at RT, followed by brief vortexing and centrifugation (1500 ***g*** for 30 sec). The pollen pellets were transferred to a glass microscope slide. To examine immature pollen grains, the anthers were isolated from developing flowers and were submerged in a drop of DAPI staining solution on a glass microscope slide. The anthers were gently squashed with a cover glass to release the pollen grains. Higher concentrations of DAPI (1.0 μg ml^{-1}) were used for staining immature pollen grains. Each slide was examined with an Axioskop (Carl Zeiss, Thornwood, NY, USA) microscope in both the epifluorescence (emission – 355 nm, excitation – 420 nm filter set) mode for nuclear configuration and the DIC optics mode. Digital images were captured and processed as above. TEM analysis (anthers from stage 10–13 flowers; Smyth *et al.*, 1990) and image processing were performed as described by Kang *et al.* (2003).

Acknowledgements

We thank R. Amasino and members of our laboratory for discussion and critical reading of the manuscript. We would also like to thank F. Schomburg for his assistance in the isolation of *adl1C-1*, J. Kimble for the generous use of her confocal microscope, J. Busse for SEM analysis of *adl1C-1* pollen, and the Electron Microscope Facility of University of Wisconsin Medical School for helping with TEM. This research was partially supported by the College of Agriculture and Life Sciences at UW-Madison, by a Department of Biochemistry predoctoral fellowship to B.-H.K., the United States Department of Agriculture Cooperative State Research Education and Extension Service Project (WIS04430), the Department of Energy, Division of Energy Biosciences (project no. DE-FG02–99ER20332), and an award from the Milwaukee Foundation to S.Y.B.

References

Achiriloaie, M., Barylko, B. and Albanesi, J.P. (1999) Essential role of the dynamin pleckstrin homology domain in receptor-mediated endocytosis. *Mol. Cell Biol.* **19**, 1410–1415.

Altschul, S.F., Madden, T.L., Schaffer, A.A., Zhang, J., Zhang, Z., Miller, W. and Lipman, D.J. (1997) Gapped BLAST and PSI-BLAST: a new generation of protein database search programs. *Nucl. Acids Res.* **25**, 3389–3402.

Arimura, S. and Tsutsumi, N. (2002) A dynamin-like protein (ADL2b), rather than FtsZ, is involved in *Arabidopsis* mitochondrial division. *Proc. Natl. Acad. Sci. USA*, **99**, 5727–5731.

Ausubel, F.M., Brent, R., Kingston, R.E., Moore, D.D., Seidman, J.G., Smith, J.A. and Struhl, K. (1989–1995) *Current Protocols in Molecular Biology.* New York: Wiley.

Axelos, M., Curie, C., Mazzolini, L., Bardet, C. and Lescure, B. (1992) A protocol for transient gene expression in *Arabidopsis thaliana* protoplasts isolated from cell suspension cultures. *Plant Physiol. Biochem.* **30**, 123–128.

Baluska, F., Hlavacka, A., Samaj, J., Palme, K., Robinson, D.G., Matoh, T., McCurdy, D.W., Menzel, D. and Volkmann, D. (2002) F-actin-dependent endocytosis of cell wall pectins in meristematic root cells. Insights from brefeldin A-induced compartments. *Plant Physiol.* **130**, 422–431.

Bar-Peled, M. and Raikhel, N.V. (1996) A method for isolation and purification of specific antibodies to a protein fused to the GST. *Anal. Biochem.* **241**, 140–142.

Battey, N.H., James, N.C., Greenland, A.J. and Brownlee, C. (1999) Exocytosis and endocytosis. *Plant Cell*, **11**, 643–660.

Bednarek, S.Y. and Falbel, T.G. (2002) Membrane trafficking during plant cytokinesis. *Traffic*, **3**, 621–629.

van der Bliek, A.M. (1999) Functional diversity in the dynamin family. *Trends Cell Biol.* **9**, 96–102.

Chen, Y.C. and McCormick, S. (1996) Sidecar pollen, an *Arabidopsis thaliana* male gametophytic mutant with aberrant cell divisions during pollen development. *Development*, **122**, 3243–3253.

Clough, S.J. and Bent, A.F. (1998) Floral dip: a simplified method for *Agrobacterium*-mediated transformation. *Plant J.* **16**, 735–743.

Donnelly, P.M., Bonetta, D., Tsukaya, H., Dengler, R.E. and Dengler, N.G. (1999) Cell cycling and cell enlargement in developing leaves of *Arabidopsis*. *Dev. Biol.* **215**, 407–419.

El-Ghazaly, G., Huysmans, S. and Smets, E. (2001) Pollen development of *Rondeletia odorata* (Rubiaceae). *Am. J. Bot.* **88**, 14–30.

Fahn, A. (1990) *Plant Anatomy. (Oxford, England).* New York: Pergamon Press.

Fei, H. and Sawhney, V.K. (2001) Ultrastructural characterization of male sterile 33 (*ms33*) mutant in *Arabidopsis* affected in pollen desiccation and maturation. *Can. J. Bot.* **79**, 118–129.

Galway, M.E., Heckman, J.W., Jr and Schiefelbein, J.W. (1997) Growth and ultrastructure of *Arabidopsis* root hairs: the *rhd3* mutation alters vacuole enlargement and tip growth. *Planta*, **201**, 209–218.

Grini, P.E., Schnittger, A., Schwarz, H., Zimmermann, I., Schwab, B., Jürgens, G. and Hülskamp, M. (1999) Isolation of ethyl methanesulfonate-induced gametophytic mutants in *Arabidopsis thaliana* by a segregation distortion assay using the multimarker chromosome 1. *Genetics*, **151**, 849–863.

Gupta, R., Ting, J.T., Sokolov, L.N., Johnson, S.A. and Luan, S. (2002) A tumor suppressor homolog, AtPTEN1, is essential for pollen development in *Arabidopsis*. *Plant Cell*, **14**, 2495–2507.

Hajdukiewicz, P., Svab, Z. and Maliga, P. (1994) The small, versatile *pPZP* family of *Agrobacterium* binary vectors for plant transformation. *Plant Mol. Biol.* **25**, 989–994.

Harlow, E. and Lane, D. (1988) *Antibodies: a Laboratory Manual.* Cold Spring Harbor, New York: Cold Spring Harbor Laboratory Press.

Hepler, P.K., Vidali, L. and Cheung, A.Y. (2001) Polarized cell growth in higher plants. *Annu. Rev. Cell Dev. Biol.* **17**, 159–187.

Heslop-Harrison, J. (1978) Recognition and response in the pollen–stigma interaction. *Symp. Soc. Exp. Biol.* **32**, 121–138.

Hoepfner, D., van den Berg, M., Philippsen, P., Tabak, H.F. and Hettema, E.H. (2001) A role for Vps1p, actin, and the Myo2p motor in peroxisome abundance and inheritance in *Saccharomyces cerevisiae*. *J. Cell Biol.* **155**, 979–990.

Holstein, S.E. (2002) Clathrin and plant endocytosis. *Traffic*, **3**, 614–620.

Homann, U. and Thiel, G. (1999) Unitary exocytotic and endocytotic events in guard-cell protoplasts during osmotically driven volume changes. *FEBS Lett.* **460**, 495–499.

Howden, R., Park, S.K., Moore, J.M., Orme, J., Grossniklaus, U. and Twell, D. (1998) Selection of T-DNA-tagged male and female gametophytic mutants by segregation distortion in *Arabidopsis*. *Genetics*, **149**, 621–631.

Kang, B.-H., Busse, J.S. and Bednarek, S.Y. (2003) Members of the *Arabidopsis* dynamin-like gene family, ADL1, are essential for

plant cytokinesis and polarized cell growth. *Plant Cell*, **15**, 899–913.

Kang, B.-H., Busse, J.S., Dickey, C., Rancour, D.M. and Bednarek, S.Y. (2001) The *Arabidopsis* cell plate-associated dynamin-like protein, ADL1a, is required for multiple stages of plant growth and development. *Plant Physiol.* **126**, 47–68.

Ketelaar, T., De Ruijter, N.C. and Emons, A.M. (2003) Unstable f-actin specifies the area and microtubule direction of cell expansion in *Arabidopsis* root hairs. *Plant Cell*, **15**, 285–292.

Kim, Y.W., Park, D.S., Park, S.C., Kim, S.H., Cheong, G.W. and Hwang, I. (2001) *Arabidopsis* dynamin-like 2 that binds specifically to phosphatidylinositol 4-phosphate assembles into a high-molecular weight complex *in vivo* and *in vitro*. *Plant Physiol.* **127**, 1243–1255.

Koch, A., Thiemann, M., Grabenbauer, M., Yoon, Y., McNiven, M.A. and Schrader, M. (2003) Dynamin-like protein 1 is involved in peroxisomal fission. *J. Biol. Chem.* **278**, 8597–8605.

Kropf, D.L., Bisgrove, S.R. and Hable, W.E. (1998) Cytoskeletal control of polar growth in plant cells. *Curr. Opin. Cell Biol.* **10**, 117–122.

Krysan, P.J., Young, J.C., Tax, F. and Sussman, M.R. (1996) Identification of transferred DNA insertions within *Arabidopsis* genes involved in signal transduction and ion transport. *Proc. Natl. Acad. Sci. USA*, **93**, 8145–8150.

Kuang, A. and Musgrave, M.E. (1996) Dynamics of vegetative cytoplasm during generative cell formation and pollen maturation in *Arabidopsis thaliana*. *Protoplasma*, **194**, 81–90.

Kubitscheck, U., Homann, U. and Thiel, G. (2000) Osmotically evoked shrinking of guard-cell protoplasts causes vesicular retrieval of plasma membrane into the cytoplasm. *Planta*, **210**, 423–431.

Lalanne, E. and Twell, D. (2002) Genetic control of male germ unit organization in *Arabidopsis*. *Plant Physiol.* **129**, 865–875.

Lam, B.C., Sage, T.L., Bianchi, F. and Blumwald, E. (2002) Regulation of ADL6 activity by its associated molecular network. *Plant J.* **31**, 565–576.

Lauber, M.H., Waizenegger, I., Steinmann, T., Schwarz, H., Mayer, U., Hwang, I., Lukowitz, W. and Jürgens, G. (1997) The *Arabidopsis* KNOLLE protein is a cytokinesis-specific syntaxin. *J. Cell Biol.* **139**, 1485–1493.

Lee, E. and De Camilli, P. (2002) Dynamin at actin tails. *Proc. Natl. Acad. Sci. USA*, **99**, 161–166.

Li, H., Lin, Y., Heath, R.M., Zhu, M.X. and Yang, Z. (1999) Control of pollen tube tip growth by a Rop GTPase-dependent pathway that leads to tip-localized calcium influx. *Plant Cell*, **11**, 1731–1742.

Lin, H.C., Barylko, B., Achiriloaie, M. and Albanesi, J.P. (1997) Phosphatidylinositol (4,5)-bisphosphate-dependent activation of dynamins I and II lacking the proline/arginine-rich domains. *J. Biol. Chem.* **272**, 25999–26004.

McCormick, S. (1993) Male gametophyte development. *Plant Cell*, **5**, 1265–1275.

McNiven, M.A., Cao, H., Pitts, K.R. and Yoon, Y. (2000) The dynamin family of mechanoenzymes: pinching in new places. *Trends Biochem. Sci.* **25**, 115–120.

Miyagishima, S.Y., Nishida, K., Mori, T., Matsuzaki, M., Higashiyama, T., Kuroiwa, H. and Kuroiwa, T. (2003) A plant-specific dynamin-related protein forms a ring at the chloroplast division site. *Plant Cell*, **15**, 655–665.

Mozo, T., Fischer, S., Shizuya, H. and Altmann, T. (1998) Construction and characterization of the IGF *Arabidopsis* BAC library. *Mol. Gen. Genet.* **258**, 562–570.

Mulholland, J., Konopka, J., Singer-Kruger, B., Zerial, M. and Botstein, D. (1999) Visualization of receptor-mediated endocytosis in yeast. *Mol. Biol. Cell*, **10**, 799–817.

Mulholland, J., Preuss, D., Moon, A., Wong, A., Drubin, D. and Botstein, D. (1994) Ultrastructure of the yeast actin cytoskeleton and its association with the plasma membrane. *J. Cell Biol.* **125**, 381–391.

Murashige, T. and Skoog, F. (1962) A revised medium for rapid growth and bioassays with tobacco tissue cultures. *Physiol. Plant.* **15**, 473–497.

Nicol, F., His, I., Jauneau, A., Vernhettes, S., Canut, H. and Höfte, H. (1998) A plasma membrane-bound putative endo-1,4-beta-D-glucanase is required for normal wall assembly and cell elongation in *Arabidopsis*. *EMBO J.* **17**, 5563–5576.

Ochoa, G.C., Slepnev, V.I., Neff, L. *et al.* (2000) A functional link between dynamin and the actin cytoskeleton at podosomes. *J. Cell Biol.* **150**, 377–389.

Orth, J.D., Krueger, E.W., Cao, H. and McNiven, M.A. (2002) The large GTPase dynamin regulates actin comet formation and movement in living cells. *Proc. Natl. Acad. Sci. USA*, **99**, 167–172.

Orth, J.D. and McNiven, M.A. (2003) Dynamin at the actin–membrane interface. *Curr. Opin. Cell Biol.* **15**, 31–39.

Owen, H.A. and Makaroff, C.A. (1995) Ultrastructure of microsporogenesis and microgametogenesis in *Arabidopsis thaliana* (L.) Heynh. ecotype Wassilewskija (Brassicaceae). *Protoplasma*, **185**, 7–21.

Park, S.K., Howden, R. and Twell, D. (1998) The *Arabidopsis thaliana* gametophytic mutation *gemini pollen 1* disrupts microspore polarity, division asymmetry and pollen cell fate. *Development*, **125**, 3789–3799.

Park, S.K. and Twell, D. (2001) Novel patterns of ectopic cell plate growth and lipid body distribution in the *Arabidopsis gemini pollen 1* mutant. *Plant Physiol.* **126**, 899–909.

Rancour, D.M., Dickey, C.E., Park, S. and Bednarek, S.Y. (2002) Characterization of AtCDC48. Evidence for multiple membrane mechanisms at the plane of cell division in plants. *Plant Physiol.* **130**, 1241–1253.

Regan, S.M. and Moffatt, B.A. (1990) Cytochemical analysis of pollen development in wild-type *Arabidopsis* and a male sterile mutant. *Plant Cell*, **2**, 877–890.

Samuels, A.L. and Bisalputra, T. (1990) Endocytosis in elongating root cells of *Lobelia erinus*. *J. Cell Sci.* **97**, 157–166.

Sanderfoot, A.A., Pilgrim, M., Adam, L. and Raikhel, N.V. (2001) Disruption of individual members of *Arabidopsis* syntaxin gene families indicates each has essential functions. *Plant Cell*, **13**, 659–666.

Sato, S., Kato, T., Kakegawa, K. *et al.* (2001) Role of the putative membrane-bound endo-1,4-beta-glucanase KORRIGAN in cell elongation and cellulose synthesis in *Arabidopsis thaliana*. *Plant Cell Physiol.* **42**, 251–263.

Schafer, D.A. (2002) Coupling actin dynamics and membrane dynamics during endocytosis. *Curr. Opin. Cell Biol.* **14**, 76–81.

Sever, S., Muhlberg, A.B. and Schmid, S.L. (1999) Impairment of dynamin's GAP domain stimulates receptor-mediated endocytosis. *Nature*, **398**, 481–486.

Smith, R.F., Wiese, B.A., Wojzynski, M.K., Davison, D.B. and Worley, K.C. (1996) BCM search launcher – an integrated interface to molecular biology database search and analysis services available on the world-wide web. *Genome Res.* **6**, 454–462.

Smyth, D.R., Bowman, J.L. and Meyerowitz, E.M. (1990) Early flower development in *Arabidopsis*. *Plant Cell*, **2**, 755–767.

Tang, W., Ezcurra, I., Muschietti, J. and McCormick, S. (2002) A cysteine-rich extracellular protein, LAT52, interacts with the extracellular domain of the pollen receptor kinase LePRK2. *Plant Cell*, **14**, 2277–2287.

Twell, D., Park, S.K., Hawkins, T.J., Schubert, D., Schmidt, R., Smertenko, A. and Hussey, P.J. (2002) MOR1/GEM1 has an

essential role in the plant-specific cytokinetic phragmoplast. *Nat. Cell Biol.* **4**, 711–714.

Twell, D., Park, S.K. and Lalanne, E. (1998) Asymmetric division and cell-fate determination in developing pollen. *Trends Plant Sci.* **3**, 305–310.

Twell, D., Yamaguchi, J., Wing, R.A., Ushiba, J. and McCormick, S. (1991) Promoter analysis of genes that are co-ordinately expressed during pollen development reveals pollen-specific enhancer sequences and shared regulatory elements. *Genes Dev.* **5**, 496–507.

Van Aelst, A.C., Pierson, E.S., Van Went, J.L. and Cresti, M. (1993) Ultrastructural changes of *Arabidopsis thaliana* pollen during final maturation and rehydration. *Zygote*, **1**, 173–179.

Whittington, A.T., Vugrek, O., Wei, K.J., Hasenbein, N.G., Sugimoto, K., Rashbrooke, M.C. and Wasteneys, G.O. (2001) MOR1 is essential for organizing cortical microtubules in plants. *Nature*, **411**, 610–613.

Wong, E.D., Wagner, J.A., Gorsich, S.W., McCaffery, J.M., Shaw, J.M. and Nunnari, J. (2000) The dynamin-related GTPase, Mgm1p, is an intermembrane space protein required for maintenance of fusion competent mitochondria. *J. Cell Biol.* **151**, 341–352.

Zheng, J., Cahill, S.M., Lemmon, M.A., Fushman, D., Schlessinger, J. and Cowburn, D. (1996) Identification of the binding site for acidic phospholipids on the pH domain of dynamin: implications for stimulation of GTPase activity. *J. Mol. Biol.* **255**, 14–21.